Results from the ALEPH experiment at LEP 2

Dr. C.N. Booth
University of Sheffield, SHEFFIELD, England

Abstract

High energy data from LEP are used to make precise measurements of parameters of the standard model, and to search for physics beyond it. W pairs are studied, enabling a number of independent measurements of the W mass and studies of W decays. Limits are presented for the masses of neutral and charged Higgs particles, while searches for supersymmetric particles have allowed significant regions of SUSY parameter space to be excluded. Lower limits on the masses of neutralinos, charginos, sleptons and squarks are presented, and supergravity and R-parity violating models are investigated.

1 Introduction

For six very successful years, LEP, the electron-positron collider at CERN, ran at energies close to the Z-mass, enabling the 4 experiments to perform high precision studies on Z^0 production and decay. In 1995, the energy was raised to intermediate values of 130 to 140 GeV, before running commenced at and above the W-pair threshold. The higher energies have been devoted primarily to studies of W-pair production and searches for new physics. Currently, LEP is running at 183 GeV, and at the time of this workshop about 14 pb^{-1} have been collected by the ALEPH experiment. The energies and integrated luminosities are summarised in table 1. Unless otherwise indicated, the results presented here were obtained from the data taken in 1996.

	Year of running	Energy	Integrated luminosity
LEP 1	1989-95	88-94 GeV	132 pb^{-1}
LEP 1.5	1995	130-140 GeV	6 pb^{-1}
LEP 2	1996	162 GeV	11 pb^{-1}
	1996	170-172 GeV	11 pb^{-1}
	1997 (to date)	183 GeV	14 pb^{-1}

Table 1: Approximate integrated luminosities used by the ALEPH experiment

The remainder of this paper presents the key features of the ALEPH apparatus, followed by some of the important physics results obtained at LEP 2. W-pair events have been identified, and used to study the mass of the W, both through direct reconstruction and from the cross-section at threshold. The cross-section measurement has been used to test the standard model, and decay branching ratios used both to verify lepton universality and to measure one of the elements of the CKM matrix. Angular variables also provide limits on non-standard triple gauge couplings. In the area of searches, results are presented on the standard model Higgs boson and on both charged and neutral Higgs of extended models. Finally, searches for a range of supersymmetric particles, including charginos, neutralinos, sleptons and squarks, are used to constrain the masses of these particles, and hence parameters of supersymmetric models. Searches in channels containing only photons and missing energy are used to investigate gauge-mediated SUSY-breaking and limits on R-parity violating models are given.

2 The ALEPH Detector

The ALEPH detector and its performance have been described in detail in references [1] and [2]. Here, only the important parameters are presented which are relevant to the physics studied in this paper – W-physics and searches for Higgs and new particles.

An important feature of ALEPH is its excellent tracking capability. This is primarily provided by a large time projection chamber. In addition to furnishing a momentum resolution which can be parametrised as $\delta P_{\mathrm{T}}/P_{\mathrm{T}}^2 = 6 \times 10^{-4}(\mathrm{GeV}/c)^{-1}$, the TPC also aids in particle identification by providing ionisation measurements. The TPC is augmented by a silicon vertex detector, which was upgraded after LEP 1 to double the angular coverage, and provides an impact parameter resolution of about $40\,\mu$m.

Around the tracking chambers is a finely-segmented electromagnetic calorimeter, which provides electron and photon identification, measuring these particles with an energy resolution of $0.18/\sqrt{E}$ (with E measured in GeV), and an angular resolution of about 1 mrad. Muons are identified both through the tracks they leave in the hadronic calorimeter and from the hits they leave in muon chambers which enclose the apparatus. Through the use of energy-flow algorithms, the hadronic energy is also well reconstructed. The angular resolution of jets is about 20 mrad while the uncertainty in their energy can be parametrised as $\sigma_{E_{\mathrm{jet}}} \approx (0.60\sqrt{E} + 0.6)\mathrm{GeV} \times (1 + \cos^2\theta)$.

In addition, the ALEPH detector is highly hermetic, with luminosity calorimeters closing the acceptance down to 35 mrad from the beam direction. This allows reliable measurement of the missing energy and momentum in events.

3 WW Physics

According to the standard model, W pairs are produced in e^+e^- annihilation through three diagrams. These involve s-channel production of a Z or a photon and t-channel exchange of an electron-neutrino. In addition, interference between these diagrams has a very significant effect. Studies of W events allow measurements of the mass and production cross section, in addition to the decay branching fractions.

3.1 W Mass Measurements

Precision measurement of this parameter is important, since the ratio of the W- and Z-masses is a test of the standard model, sensitive to new physics. The W mass has been measured by ALEPH in a number of ways, with different systematic errors.

3.1.1 Direct Measurement at 172 GeV

Ws can decay leptonically, into a charged lepton and neutrino, or hadronically into a pair of quarks. The W pair can thus be seen as a leptonic, semi-leptonic or hadronic final state. For this study, the leptonic mode is not used, as the two invisible neutrinos prevent a sufficiently accurate reconstruction. In the hadronic case, quark 4-vectors are reconstructed from the observed jets.

The precise event selection cuts are described in [3]. For the hadronic channel, the dominant backgrounds are from Z decay to a quark-antiquark pair and Z-pair production leading to 4 jets. Initial cuts are made on the missing energy, sphericity and thrust of the event. Selection is then made using a 21-variable neural network, trained using appropriate signal and background Monte Carlo samples. An efficiency of 82% is achieved for a purity of 77%. To identify the decaying Ws, jets are paired to yield the smallest difference in di-jet mass. The W mass is determined by performing a 4-constraint fit, imposing energy and momentum conservation. Rescaling is employed to give W velocities consistent with the measured masses, and two masses are calculated per event.

The semileptonic events are selected on the basis of the energy and isolation of the identified lepton and the missing transverse energy. In the case of electrons, the energy is corrected for visible bremsstrahlung. Finally, one mass per event is obtained by performing a 5C fit with an equal mass constraint. The efficiency, purity and number of events selected in each channel is given in table 2.

	qqqq	$(e/\mu)\nu$qq	$\tau\nu$qq
efficiency	77%	85%	54%
purity	80%	98%	94%
Number selected	65	34	10

Table 2: Overall efficiency and purity of W-pair event selection, with number of events selected.

In order to determine the W mass, a fit must be performed to the individual masses measured above. The Breit-Wigner distribution is distorted by phase-space, detector resolution, selection cuts and radiative losses. A fit is therefore performed to the distribution obtained from Monte Carlo events, as is shown, in the case of hadronic events, in figure 1. Combining results from hadronic and semi-leptonic decays, after a careful study of systematic errors (including colour reconnection and Bose Einstein effects), yields a mass measurement of $M_{\mathrm{W}} = 80.80 \pm 0.32 \pm 0.10\,\mathrm{GeV}/c^2$.

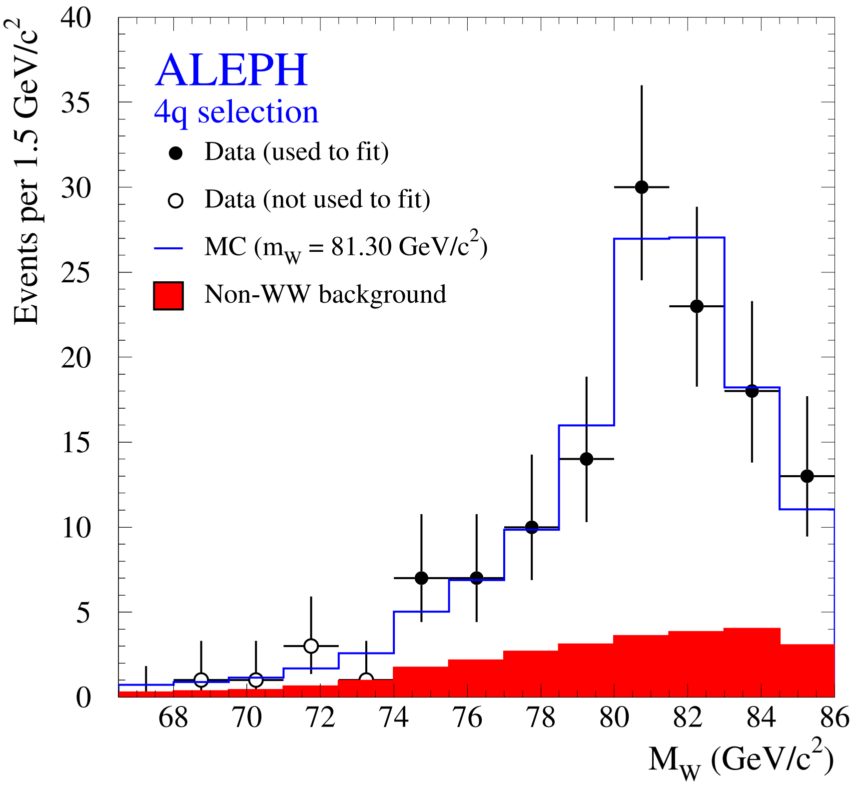

Figure 1: Mass distribution for hadronic data (points), background Monte Carlo (shaded) and signal+background Monte Carlo for the best fit to the data (line).

3.1.2 Threshold Measurement at 161 GeV

At centre-of-mass energies close to twice the W mass, the cross-section for the production of a W pair depends critically on the exact value of that mass. For this study, leptonic, semileptonic and hadronic channels are used, and the selected W-pair events at 161 GeV yield the individual channel cross-sections listed in table 3 [4]. These cross-sections are combined, applying the constraint of fixing the branching ratios to their standard model values, and imply a cross-section for W pair production of $\sigma_{\mathrm{WW}} = 4.23 \pm 0.73 \pm 0.19\,\mathrm{pb}$. The GENTLE program [5] is used to calculate the standard model cross-section as a function of W mass and centre-of-mass energy, and hence the mass of the W is determined as $M_{\mathrm{W}} = 80.14 \pm 0.34 \pm 0.09 \pm 0.03$ GeV/c^2, where the third error quoted is due to the uncertainty in the energy of LEP.

161 GeV		
$\sigma(\mathrm{WW} \to l\nu l\nu)$	$=$	$0.68\,^{+0.34}_{-0.26} \pm 0.03$ pb
$\sigma(\mathrm{WW} \to l\nu \mathrm{qq})$	$=$	$1.85\,^{+0.51}_{-0.43} \pm 0.06$ pb
$\sigma(\mathrm{WW} \to \mathrm{qqqq})$	$=$	$1.80 \pm 0.50 \pm 0.19$ pb
σ_{WW}	$=$	$4.23 \pm 0.73 \pm 0.19$ pb
172 GeV		
$\sigma(\mathrm{WW} \to l\nu l\nu)$	$=$	$1.22\,^{+0.46}_{-0.37} \pm 0.07$ pb
$\sigma(\mathrm{WW} \to l\nu \mathrm{qq})$	$=$	$1.85 \pm 0.76 \pm 0.16$ pb
$\sigma(\mathrm{WW} \to \mathrm{qqqq})$	$=$	$5.76 \pm 1.23 \pm 0.25$ pb
σ_{WW}	$=$	$11.71 \pm 1.23 \pm 0.25$ pb

Table 3: Cross-Sections for W Production and Decay at 161 and 172 GeV

3.1.3 W Cross-Section at 172 GeV

The WW production cross-sections are determined at 172 GeV using the same method as outlined above, and are also listed in table 3 [6]. In this case, rather than using the data to determine the W mass, we can use them to test the standard model. Figure 2 compares ALEPH's measurements of the cross-section at 161 and 172 GeV, together with a preliminary value from 183 GeV, with three models, in each case using the world average value of the W mass available before LEP 2. The solid lines show the prediction of the standard model with all three diagrams contributing; the range of values indicated is a result of the uncertainty in the W mass. The dotted line shows the expectation with no ZWW coupling, while the dashed line gives the cross-section with neither of the s-channel diagrams. It is clear that the standard model is strongly favoured by the ALEPH measurements, and the highest energy result is certainly not compatible with the alternative lines.

Combining the 161 and 172 GeV cross-section measurements, the GENTLE program is again used to determine a value for the W mass of $M_{\mathrm{W}} = 80.20 \pm 0.33 \pm 0.09 \pm 0.03\,\mathrm{GeV}/c^2$. When combined with the direct mass measurement at 172 GeV, ALEPH's best value for the mass of the W to date is $M_{\mathrm{W}} = 80.51 \pm 0.24\,\mathrm{GeV}/c^2$. A summary of the various ALEPH measurements is presented in figure 3, which also shows the standard model prediction as a function of the top and Higgs masses. Our result is clearly consistent with the standard model, and for $m_{\mathrm{t}} = 175 \pm 6$ GeV/c^2 weakly favours a light Higgs.

3.2 W Decays

Using the above leptonic and semileptonic decays of the W from the 172 GeV data, the leptonic branching ratios are determined [6]. As shown in table 4, they are all in excellent agreement with the standard model value of 10.8%. If lepton universality is assumed, the hadronic branching fraction is more tightly constrained, and determined to be $67.7 \pm 3.1 \pm 0.7\%$, which may be compared with the standard model value of 67.5%. This branching fraction may be written as

$$B(\mathrm{W} \to \mathrm{hadrons}) = \frac{|\mathrm{V_{ud}}|^2 + |\mathrm{V_{cd}}|^2 + |\mathrm{V_{us}}|^2 + |\mathrm{V_{cs}}|^2 + |\mathrm{V_{ub}}|^2 + |\mathrm{V_{cb}}|^2}{1 + \sum_{ij} |\mathrm{V}_{ij}|^2} \times \left(1 + \frac{\alpha_{\mathrm{S}}(M_{\mathrm{W}}^2)}{3\pi}\right).$$

Most of the CKM matrix elements entering the sum are already well determined; an exception is $\mathrm{V_{cs}}$. We can therefore use ALEPH's measurement of the hadronic branching fraction to determine $|\mathrm{V_{cs}}| = 0.98 \pm 0.14 \pm 0.03$. This is consistent with, but also improves upon, the published value determined from studies of D decays, of $|\mathrm{V_{cs}}| = 1.01 \pm 0.18$ [7].

ALEPH can also measure $\mathrm{V_{cs}}$ directly, from W decays to charmed particles. The latter are tagged with a neural network on the basis of jet shape, large impact parameters and the presence of energetic leptons [8]. As a result, the hadronic branching fraction into charm is determined as $0.57 \pm 0.18 \pm 0.04$, implying a value of $|\mathrm{V_{cs}}| = 1.13 \pm 0.43 \pm 0.03$. Clearly, this method results in a value with significantly

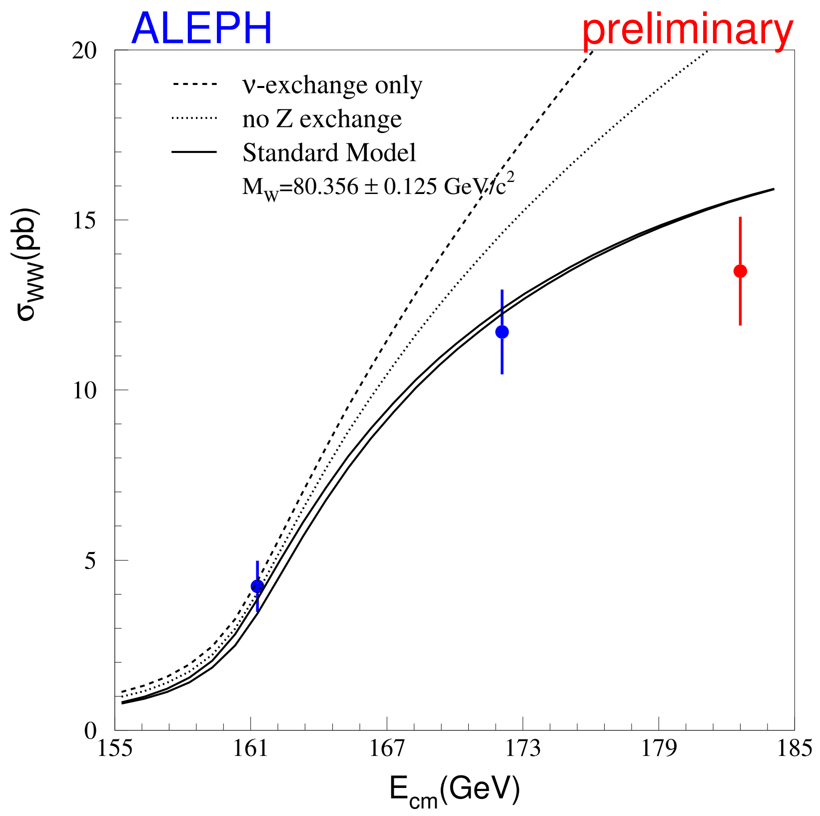

Figure 2: Comparison of the measured W-pair production cross-section with the Standard Model prediction from GENTLE for the world average value of the W mass. Also shown are predicted cross-sections from the t-channel neutrino exchange diagram alone and from also including s-channel photon exchange but no Z exchange.

larger statistical errors, though it should be pointed out that it does not assume the validity of the standard model.

3.3 Triple Gauge Couplings

Triple gauge couplings form an essential part of the standard model, and the investigation of their forms is one of the primary motivations for LEP 2. For each of the ZWW and γWW diagrams, there could, in the most general case, be 7 independent couplings, making 14 parameters in all. Some combinations of these couplings are poorly constrained by the measurements performed at LEP 1 and lower energies. These couplings are conventionally parametrised in terms of three variables $\alpha_{\mathrm{w}\phi}$, $\alpha_{\mathrm{b}\phi}$ and α_{w} which are zero in the standard model, and which are determined by performing fits to the following angular distributions in W-pair events [9]: the production angle of the W^-, the polar decay angles in the $\mathrm{W}^\pm$ rest frames and the azimuthal decay angles with respect to the plane containing the $\mathrm{W}^\pm$ and the beam. Given the present low statistics, three independent fits are performed, in each case determining the value of one of the coupling parameters while fixing the other two to zero. The results obtained are $\alpha_{\mathrm{w}\phi} = 0.14\,^{+0.27+0.11}_{-0.25-0.12}$, $\alpha_{\mathrm{w}} = 0.06\,^{+0.58+0.12}_{-0.52-0.12}$ and $\alpha_{\mathrm{b}\phi} = 1.01\,^{+0.86+0.29}_{-2.14-0.33}$. Clearly, the values are as yet not tightly constrained, but it can be seen in all cases that they are consistent with the standard model expectation of zero.

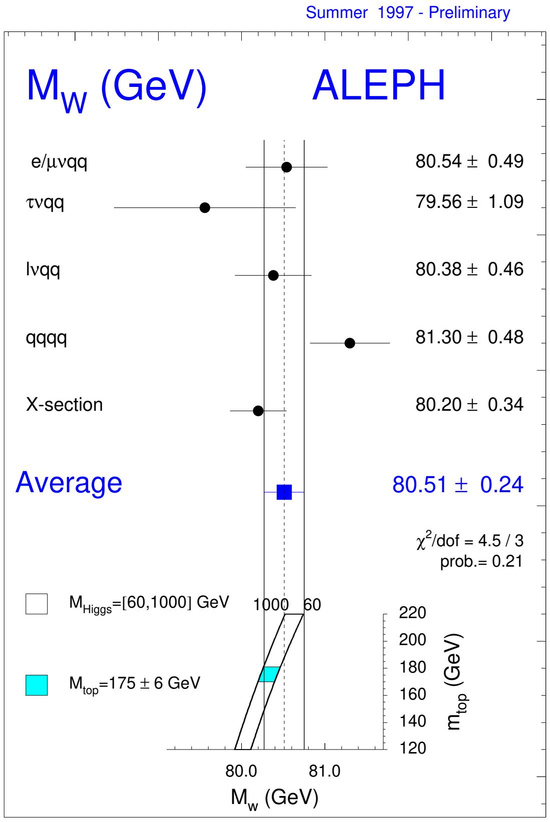

Figure 3: Summary of ALEPH's W mass measurements, and comparison with the Standard Model expectation as a function of top and Higgs mass.

4 Higgs Searches

The Standard Model contains a doublet of complex scalar fields resulting, after symmetry breaking, in a single neutral Higgs boson H^0. In models with an additional doublet, 5 scalar physical states exist, denoted H^0, $H^{\pm}$, h and A. ALEPH has conducted searches for all these particles, and here are presented searches for the standard model Higgs, charged Higgs and the neutral Higgs of the minimal supersymmetric model (MSSM).

4.1 Standard Model Higgs Search

The dominant process leading to the production of a Higgs at LEP 2 is the production of a virtual Z which subsequently decays to a real Z and a Higgs. The cross-section is large for Higgs masses up to the centre-of-mass energy minus the Z mass, giving a reach of 80 GeV for $\sqrt{s} = 172\,\mathrm{GeV}$. (Production of e^+e^- or $\bar{\nu}\nu$ via t-channel exchange of a Z or W with subsequent emission of a Higgs from the boson has in principle a higher reach, but a very much smaller cross-section.) The observed final states are then a result of the Z decaying to e^+e^-, $\mu^+\mu^-$, $\tau^+\tau^-$, $\bar{\nu}\nu$ or $q\bar{q}$ and the Higgs decaying to $b\bar{b}$, $\tau^+\tau^-$, $c\bar{c}$ or gg.

The selection for such states is optimised using signal and background Monte Carlo samples [10]. As an example, the $l^+l^-b\bar{b}$ decay mode is described here. Two isolated or identified leptons are required, and in order to tag the production of a Z, their invariant mass (together with possible bremsstrahlung photons in the case of electrons) is required to be at least $80\,\mathrm{GeV}/c^2$. (This cut is made tighter if only one of the candidate leptons is identified.) To remove radiative returns to the Z, events with a photon

$B(\mathrm{W} \to \mathrm{e}\nu)$	=	$9.7^{+2.1}_{-1.9} \pm 0.5$ %
$B(\mathrm{W} \to \mu\nu)$	=	$11.2^{+2.1}_{-1.9} \pm 0.6$ %
$B(\mathrm{W} \to \tau\nu)$	=	$11.3^{+2.8}_{-2.6} \pm 0.6$ %
$B(\mathrm{W} \to \mathrm{hadrons})$	=	$67.7 \pm 3.1 \pm 0.7$ %

Table 4: Measured leptonic and derived hadronic branching ratios

of energy greater than 45 GeV are vetoed. The Durham algorithm [11] is then used to force remaining particles into two jets, and the dijet mass is required to be greater than 15 GeV/c^2. This cut removes $\mathrm{e}^+\mathrm{e}^-\gamma^*$ and $\mathrm{Z}\gamma^*$ events. Finally, in order to veto W-pair events, cases with only one identified lepton are rejected if they are compatible with $\mathrm{e}^+\mathrm{e}^- \to \mathrm{WW} \to l\nu\mathrm{qq}$. At $\sqrt{s} = 172$ GeV, this results in an efficiency of about 75% for a Higgs of mass 70 GeV/c^2, and an expected background of 0.2 events. No candidate events are seen. Limits from all the decay channels are combined, excluding at 95% confidence level the range $45 < M_\mathrm{H} < 69.4$ GeV/c^2. When combined with ALEPH's published results from LEP 1[12], the lower mass interval is also excluded and a 95% confidence level limit of $M_\mathrm{H} > 70.7$ GeV/c^2 is set. (All limits in this paper are quoted at the 95% confidence level unless otherwise stated.) A preliminary result from extending the above analysis to include the data taken to date at 183 GeV improves this lower limit to 74.0 GeV/c^2.

4.2 Charged Higgs Search at 130-172 GeV

The predominant decays of a charged Higgs are $\mathrm{H}^+ \to \mathrm{c\bar{s}}$ and $\mathrm{H}^+ \to \tau^+\nu_\tau$. A search is therefore performed for final states compatible with production of $\mathrm{c\bar{s}s\bar{c}}$, $\mathrm{c\bar{s}}\tau^-\bar{\nu_\tau}$ (and charge-conjugate) or $\tau^+\nu_\tau\tau^-\bar{\nu_\tau}$. The major background to this process arises from W-pairs, which can decay to identical sets of particles.

Selections for the leptonic and semi-leptonic channels are based on a large missing energy with isolated, reconstructed τ and isolated ν[13]. In the semi-leptonic case, it is required that the dijet mass be less than 70 GeV/c^2. For events consistent with 4 jets, cuts are applied on visible energy, thrust and missing longitudinal momentum, and events with photon-like jets are rejected. Energies are then rescaled to conserve 4-momentum, and events are only accepted if jets can be paired such that the two dijet masses are equal within 10 GeV/c^2. A veto is then applied if another pairing of the jets results in a dijet mass within 2 GeV/c^2 of the W mass. Finally, a 5C fit is performed with an equal dijet mass constraint.

Overall, 15 events are selected from the 130 to 172 GeV data, with an expected background of 23.3. Limits are thus set as a function of the Higgs mass M_H and the leptonic branching ratio $BR(\mathrm{H} \to \tau\nu)$, as is shown in figure 4. As can be seen from the figure, it is possible to exclude a large mass range independent of branching ratio, and so set the limit $M_{\mathrm{H}^+} > 52$ GeV/c^2.

4.3 Neutral Higgs Bosons of the Minimal Supersymmetric Model, h and A

In the MSSM, the h and A are the lightest Higgs bosons. Two processes lead to their production: $\mathrm{e}^+\mathrm{e}^- \to \mathrm{hZ}$ with a cross-section proportional to $\sin^2(\beta-\alpha)$ and $\mathrm{e}^+\mathrm{e}^- \to \mathrm{hA}$ with a cross-section proportional to $\cos^2(\beta-\alpha)$. (The supersymmetry parameters β and α are defined in section 5.) The former case is already covered by the standard model Higgs search, and a special selection is developed for the second case[14]. A search is performed for the processes $\mathrm{e}^+\mathrm{e}^- \to \mathrm{hA} \to \mathrm{b\bar{b}b\bar{b}}, \tau^+\tau^-\mathrm{b\bar{b}}$, yielding states rich in b-jets. Tagging of b quarks can be performed on the basis of their lifetime (yielding non-zero impact parameters and reconstructed secondary vertices) and the production of leptons with a large momentum transverse to the jet axis. These two methods are combined using a neural network. Thus the $\mathrm{b\bar{b}b\bar{b}}$ final state is isolated as 4-jet events with a very high b content. The $\tau^+\tau^-\mathrm{b\bar{b}}$ selection has already been discussed, utilising missing energy, missing transverse momentum and an identified electron, muon or τ-triplet.

Combining the two selections, no events are retained, consistent with 0.91 events expected from standard model processes. An exclusion limit is therefore set in the $(M_\mathrm{h}, \sin^2(\beta-\alpha))$ plane, as shown

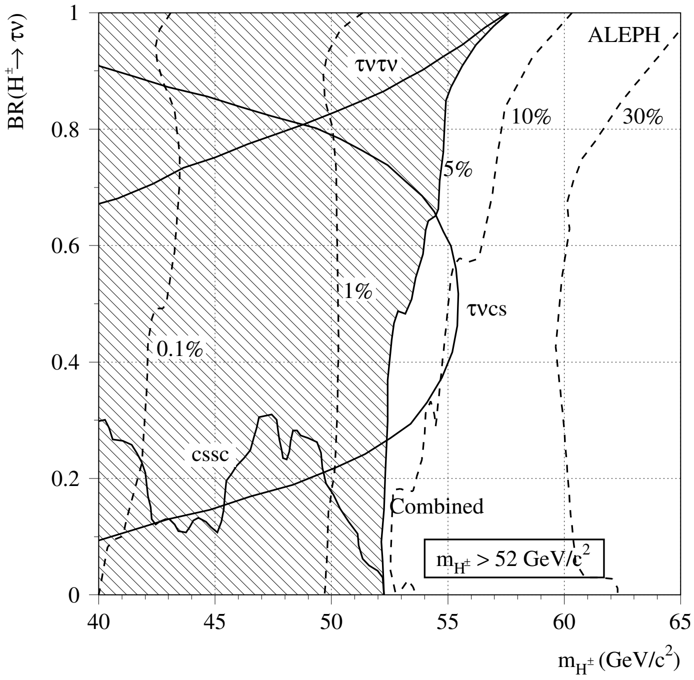

Figure 4: 95% confidence level limit on the mass of the charged Higgs boson as a function of branching ratio. The three full lines show the domains excluded by each of the three single analyses, and the hatched area is excluded by the combination of all three channels. (The dashed lines indicate other combined confidence level values.)

in figure 5a. In the most favourable case of $\cos^2(\beta-\alpha)=1$, neutral Higgs masses up to $62.5\,\mathrm{GeV}/c^2$ are excluded. These results can also be combined with those of the standard model Higgs search and a new exclusion region determined, as shown in 5b. Here it can be seen that the limit of $M_\mathrm{h} > 62.5\,\mathrm{GeV}/c^2$ applies for any value of $\cos^2(\beta-\alpha)$. The above results can also be presented as an excluded region in the $(M_\mathrm{h}, \tan\beta)$ plane. This is shown in figure 6, where the shaded area is excluded by these ALEPH measurements and the dark area is excluded by theory. The latter depends on SUSY parameters including the stop mixing – the dark area corresponds to the least favourable case of no mixing, while maximal mixing is shown by a dot-dashed line.

If $\tan\beta$ has a value greater than 1, then the ALEPH results require both M_h and M_A to be greater than $62.5\,\mathrm{GeV}/c^2$. (Preliminary results incorporating the 183 GeV data already analysed at the time of this meeting raise all the above limits by $2\,\mathrm{GeV}/c^2$ to $64.5\,\mathrm{GeV}/c^2$.)

5 Searches for Supersymmetry

In supersymmetric theories, the normal particles have partners differing in spin by one half. The partners of the fermions are known as sleptons ($\tilde{l}$) and squarks ($\tilde{\mathrm{q}}$), and since the fermions exist in both left- and right-handed forms, two sfermions exist as partners to each normal fermion, denoted $\tilde{\mathrm{f}}_\mathrm{L}$ and $\tilde{\mathrm{f}}_\mathrm{R}$. As discussed in section 4, an extra Higgs doublet results in four additional Higgs particles, the h, A and $\mathrm{H}^\pm$. The partners of the gauge bosons, known as gauginos, mix with the partners of the Higgs, the Higgsinos, to form physical states known as charginos, $\chi^\pm$, and neutralinos, χ, χ', χ'' etc.

In the minimal supersymmetric model (MSSM) masses and couplings may be defined in terms of a set of parameters including the supersymmetric mass scale μ, β where $\tan\beta = v_2/v_1$ (the ratio of the vacuum expectation values of the Higgs doublets), the mass of scalar particles at the GUT scale m_0, the

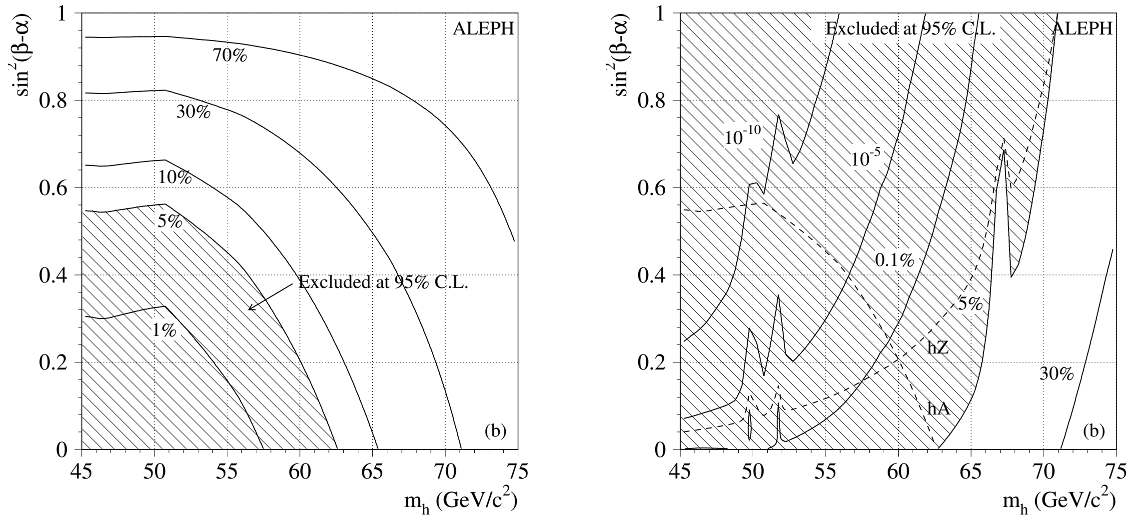

Figure 5: Confidence levels in the $(M_{\rm h}, \sin^2(\beta-\alpha))$ plane: (a) obtained from the hA search. (b) from a combination of hA and hZ analyses (solid curves) with the individual 95% confidence level results shown as dashed lines.

SU(2) gaugino mass parameter M_2 and the mixing angle α between CP-even Higgs particles h and $\rm H^0$.

ALEPH has performed searches for a number of these supersymmetric particles, both directly and indirectly, and also used the results to constrain parameters of the model. It is normally assumed that "R-parity" is conserved, that is supersymmetric particles are always produced in pairs, and the decay of unstable SUSY particles always leads to the production of the lightest supersymmetric particle (LSP), usually taken to be the χ or $\tilde{\nu}$. However, a search has also been performed in the context of models where the LSP is a gravitino (the partner of the graviton), and tests have been performed of R-parity violating supersymmetry.

5.1 Search for Charginos and Neutralinos

In $\rm e^+e^-$annihilation, chargino pairs can be produced via s-channel annihilation through a Z or photon or t-channel exchange of a $\tilde{\nu}$. Neutralino pairs ($\chi\chi$, $\chi\chi'$, $\chi'\chi'$ etc) are also produced via s-channel Z or t-channel $\tilde{\rm e}$ exchange. (For neutralinos, the diagrams interfere constructively, while for charginos the interference is destructive.) Assuming R-parity is conserved, the expected decays are then $\chi^\pm \to \chi l\nu$ or $\chi \rm q\bar{q}$ and $\chi' \to \chi l\bar{l}$, $\chi\nu\bar{\nu}$ or $\chi\rm q\bar{q}$. The signature is thus missing energy together with acoplanar jets and/or leptons. The exact search strategy depends on ΔM, defined as $M_{\chi'} - M_\chi$ or $M_{\chi^\pm} - M_\chi$ as appropriate. Monte Carlo samples have been used to optimise cuts[15] for present integrated luminosities. After this, about 11 background events are expected and 15 events selected. Limits can then be derived for assumed values of SUSY parameters. For example, figure 7 shows the 95% C.L. upper limit on the chargino pair production cross-section as a function of M_χ and $M_{\chi^\pm}$ assuming $\mu = -500\,{\rm GeV}/c^2$ and $\tan\beta = \sqrt{2}$. This can be interpreted in terms of excluded regions of μ, M_2 etc, as shown in figures 8 and 9. The lower mass limit is thus set at $85.5\,{\rm GeV}/c^2$ for gaugino-like charginos and $85.0\,{\rm GeV}/c^2$ for Higgsino-like charginos, assuming sneutrinos are heavy and taking $\tan\beta = \sqrt{2}$.

5.2 Slepton Search at 161 and 172 GeV

Sleptons will decay via $\tilde{l} \to l\chi$ (or via a cascade to a final state including these particles). The signature for slepton pairs is therefore an acoplanar lepton pair accompanied by missing energy and momentum. The details of the optimum selection[16] and the resulting efficiency depend on the $\tilde{l} - \chi$ mass difference.

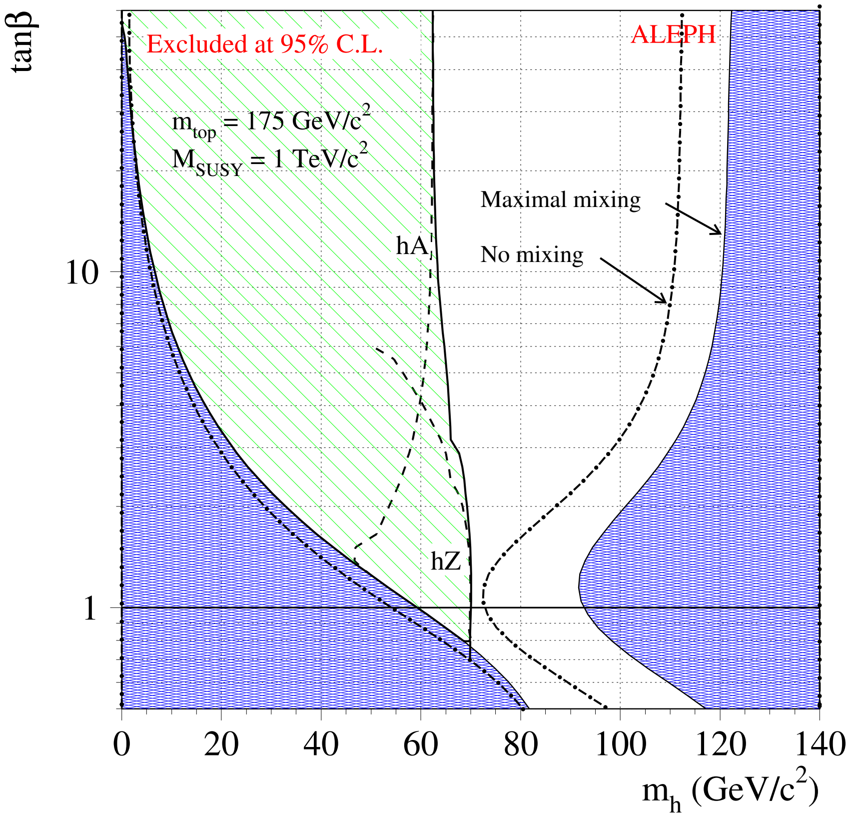

Figure 6: Excluded region in the $(M_{\mathrm{h}}, \tan\beta)$ plane. Dark areas are theoretically disallowed (for maximal stop mixing). Hatched area is excluded at the 95% confidence level by the combined search for hZ and hA. The dot-dashed lines show the change in the theoretically excluded region assuming no stop mixing.

For the large mass-difference selection, 3 candidates were found, all compatible with either $\mathrm{Z}\gamma^*$ or WW events; for small mass difference 5 candidates compatible with $\gamma\gamma$ or WW were obtained. Thus a total of 8 events were obtained, with an expected background of 7. These were combined with data similarly obtained at 130–136 GeV to obtain the exclusion plots shown in figure 10. The area above the diagonal line is excluded by the assumption that the neutralino is the LSP; a non-excluded region close to the diagonal persists due to the inability to identify events efficiently for very small $\tilde{l} - \chi$ mass differences. Providing assumptions are made to exclude this region, significant slepton mass limits can be set. For example, taking $\tan\beta = 2$ and $\mu = -200\,\mathrm{GeV}/c^2$ then: $M_{\tilde{\mu}_R} > 59\,\mathrm{GeV}/c^2$ providing $M_{\tilde{\mu}_R} - M_\chi > 10\,\mathrm{GeV}/c^2$; $M_{\tilde{\tau}_R} > 53\,\mathrm{GeV}/c^2$ providing $M_\chi < 200\,\mathrm{GeV}/c^2$; $M_{\tilde{e}_R} > 58\,\mathrm{GeV}/c^2$ providing $M_{\tilde{e}_R} - M_\chi > 3\,\mathrm{GeV}/c^2$ or $M_{\tilde{e}_R} > 75\,\mathrm{GeV}/c^2$ providing $M_{\tilde{e}_R} - M_\chi > 35\,\mathrm{GeV}/c^2$. If mass-degenerate sleptons are assumed, the lower limit on their mass is $76\,\mathrm{GeV}/c^2$ providing $M_\chi < 35\,\mathrm{GeV}/c^2$. These limits take in to account an expected inefficiency due to cascade decays.

Assuming a unification of the scalar masses at the GUT scale, the masses of the scalar particles are related at the electroweak scale[17], and for sleptons we have

$$
\begin{aligned}
M^2_{\tilde{l}_{\mathrm{R}}} &= m_0^2 + 0.22 M_2^2 - \sin^2\theta_{\mathrm{W}} M_{\mathrm{Z}}^2 \cos 2\beta \\
M^2_{\tilde{l}_{\mathrm{L}}} &= m_0^2 + 0.75 M_2^2 - 0.5(1 - 2\sin^2\theta_{\mathrm{W}}) M_{\mathrm{Z}}^2 \cos 2\beta \\
M^2_{\tilde{\nu}} &= m_0^2 + 0.75 M_2^2 + M_{\mathrm{Z}}^2 \cos 2\beta
\end{aligned}
$$

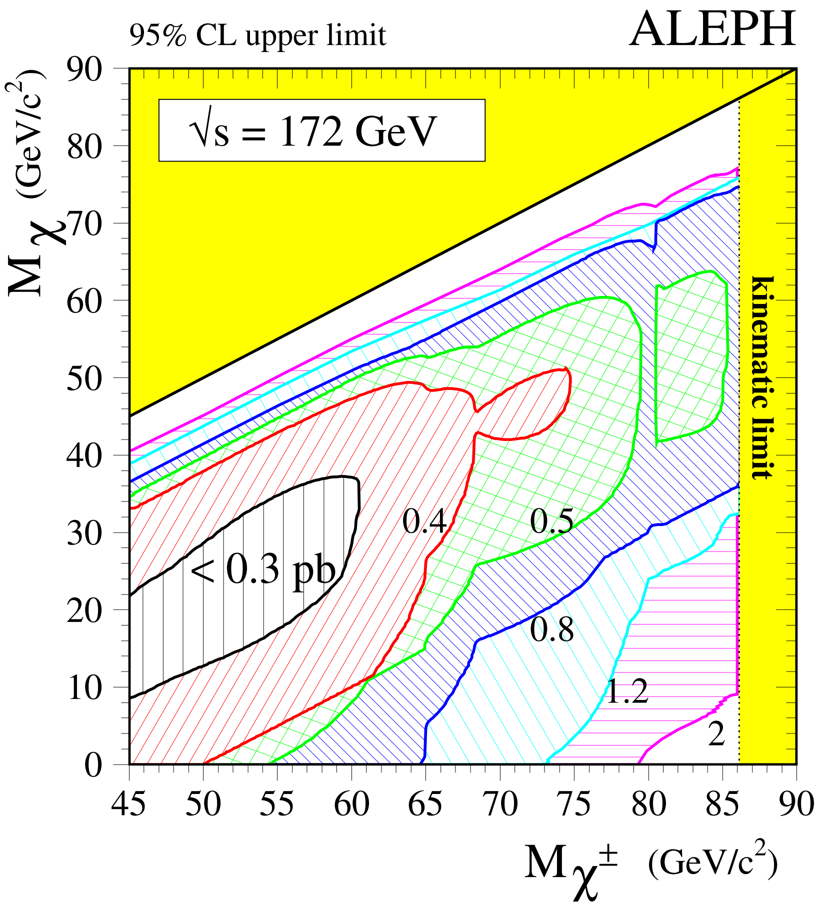

Figure 7: The 95% upper limit on the chargino pair production cross-section in the $(M_{\chi^\pm}, M_\chi)$ plane.

Using these relations, the ALEPH limits can be interpreted as an excluded region in the (m_0, M_2) plane, as is shown in figure 11. As can be seen, the LEP 2 results represent a substantial improvement on those obtained at lower energies.

5.3 Limits on the Lightest Neutralino

The results of searches for charginos, neutralinos, sleptons and neutral Higgs particles have been used to constrain the parameters of the MSSM [18]. This in turn can be used to place an indirect limit on the mass of the lightest neutralino χ (which is not directly detectable if R-parity is conserved). Under the assumption that sleptons are heavy, the $\chi^\pm$ and χ' must decay through the W and Z, and limits on the mass of the neutralino as a function of $\tan\beta$ are obtained as shown in figure 12. In this case, values of M_χ less than $25\,\mathrm{GeV}/c^2$ are excluded for all $\tan\beta > 1$. If, on the other hand, the $\tilde{l}$ and $\tilde{\nu}$ are light, and so participate in decays, the appropriate limits are those shown in figure 13a (the different lines corresponding to various values of m_0). In this case, the lower limit is given by $M_\chi > 14\,\mathrm{GeV}/c^2$ for any value of $M_{\tilde{\nu}}$ and $\tan\beta$. The limit is shown as a function of m_0 in figure 13b.

5.4 Searches for $\tilde{\mathrm{t}}$ and $\tilde{\mathrm{t}}$ squarks

Mixing between $\tilde{\mathrm{t}}_\mathrm{L}$ and $\tilde{\mathrm{t}}_\mathrm{R}$ is expected to lead to light and heavy stop squarks. This implies that the light stop could be the lightest charged SUSY particle. Searches are performed for the following decays: $\tilde{\mathrm{t}} \to \mathrm{c}\chi$, $\tilde{\mathrm{t}} \to \mathrm{b}l\tilde{\nu}$ and $\tilde{\mathrm{b}} \to \mathrm{b}\chi$, where the common signature is the large missing energy and momentum. The details of the search depend on the mass difference between the squark and the LSP, and are described

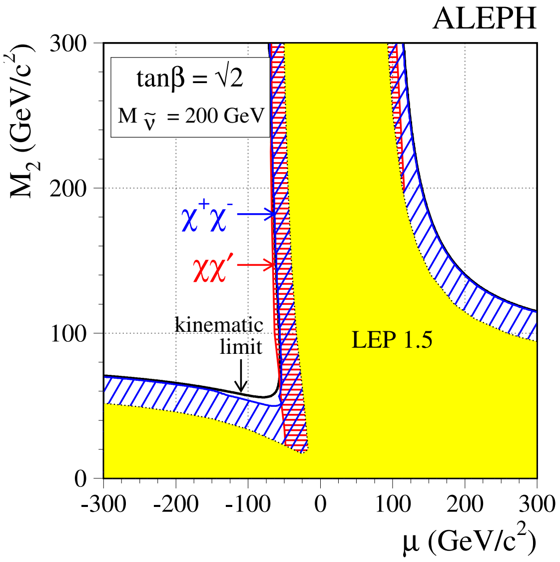

Figure 8: Excluded region in the (μ, M_2) plane for $\tan\beta = \sqrt{2}$ and 35, and $M_{\tilde{\nu}} = 200\,\mathrm{GeV}/c^2$.

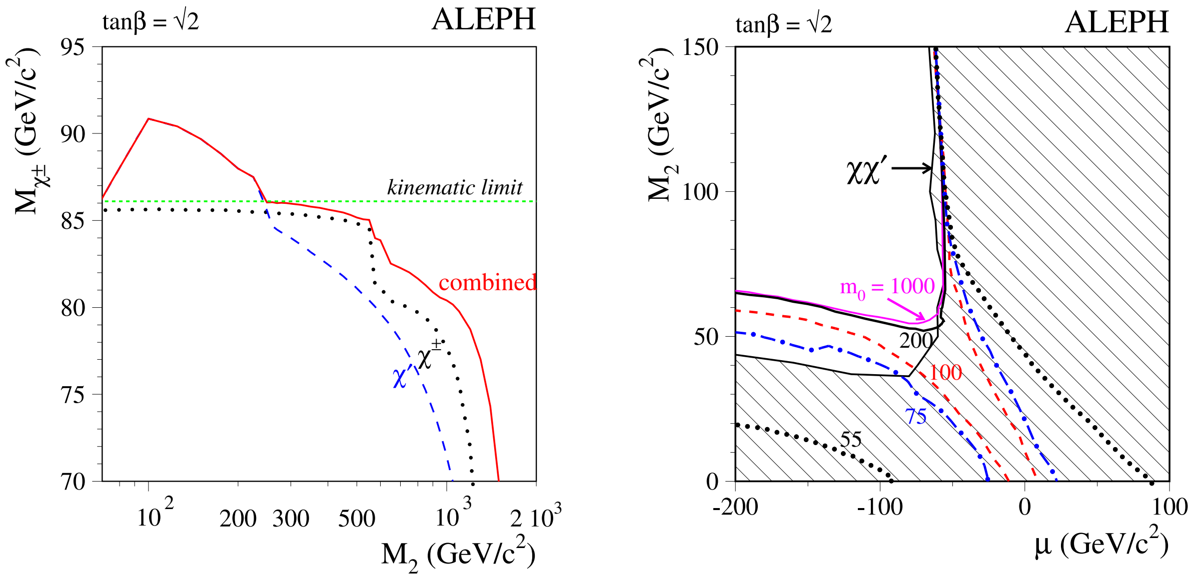

Figure 9: (a) Limit on the chargino mass as a function of M_2, from the chargino search, neutralino search and their combination. (b) Exclusion in the (μ, M_2) plane; lines indicate limits from chargino searches for several values of m_0; the hatched area is the exclusion from the neutralino analysis, for $m_0 = 75\,\mathrm{GeV}/c^2$. (The values in both figures are derived assuming $\tan\beta = \sqrt{2}$.)

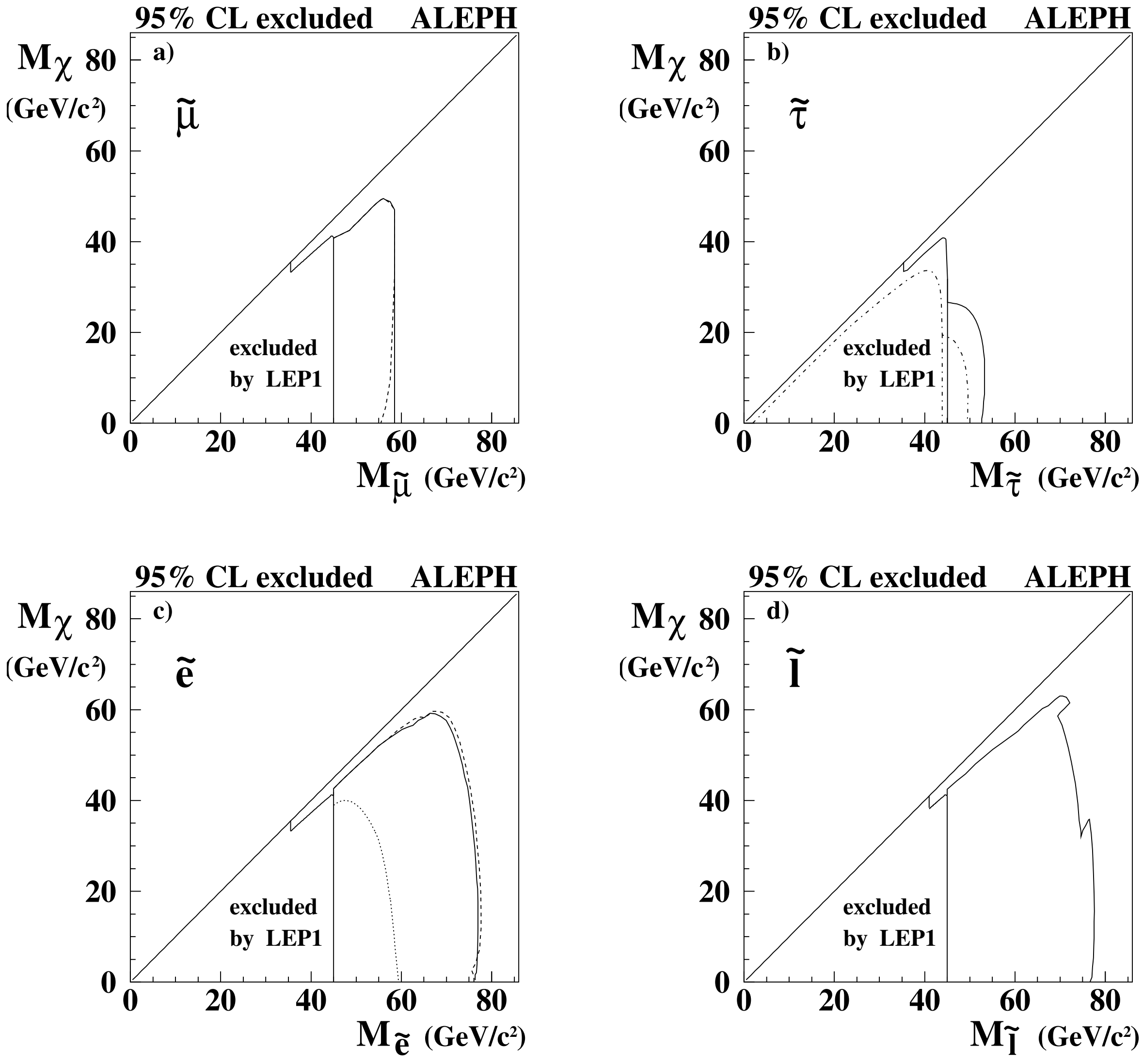

Figure 10: Excluded regions in the $(M_{\tilde{l}_R}, M_\chi)$ plane for (a) $\tilde{\mu}_R$, (b) $\tilde{\tau}_R$, (c) $\tilde{e}_R$ and (d) combined limit for mass degenerate sleptons. The dashed curves show the effects of cascade decays, for which no efficiency is assumed, for $\tan\beta = 2$ and $\mu = -200\,\mathrm{GeV}/c^2$.

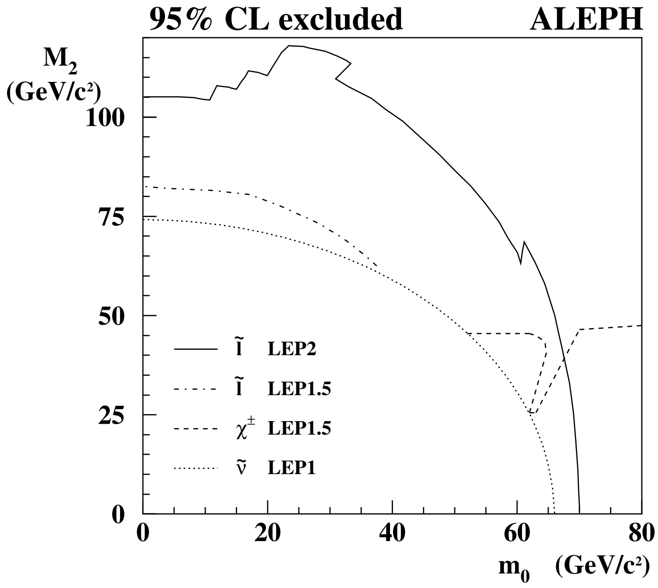

Figure 11: Limit in the (m_0, M_2) plane combining selectrons and smuons for $\tan\beta = 2$ and $\mu = -200\,\mathrm{GeV}/c^2$ (solid line). The dotted and dashed lines show earlier ALEPH results for sleptons, charginos and sneutrinos.

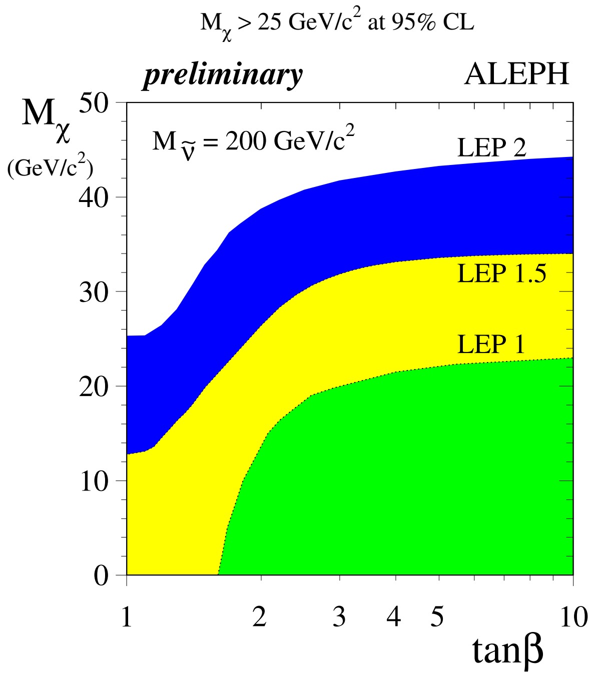

Figure 12: Lower limit on the mass of the lightest neutralino as a function of $\tan\beta$, assuming $M_{\tilde{\nu}} \geq 200\,\mathrm{GeV}/c^2$.

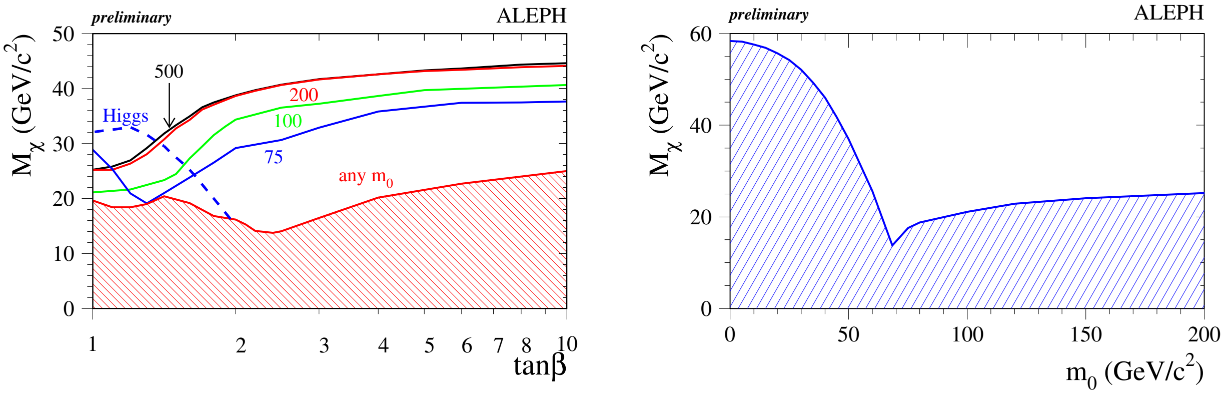

Figure 13: Lower limits on the mass of the lightest neutralino (a) as a function of $\tan\beta$ for a series of m_0 values; (b) as a function of m_0 independent of $\tan\beta$.

in [19]. One candidate is selected, consistent with the expected background of 2.2 events. The mass limits which can be deduced depend on the mixing angles $\theta_{\tilde{t}}$ and $\theta_{\tilde{b}}$, and are given in [19]. For any value of $\theta_{\tilde{t}}$, we can exclude $M_{\tilde{t}} < 67\,\mathrm{GeV}/c^2$ for the decay $\tilde{t} \to c\chi$ providing $\Delta M_{\tilde{t}\chi} > 10\,\mathrm{GeV}/c^2$ and $M_{\tilde{t}} < 68\,\mathrm{GeV}/c^2$ for the decay $\tilde{t} \to cl\tilde{\nu}$ providing $\Delta M_{\tilde{t}\tilde{\nu}} > 10\,\mathrm{GeV}/c^2$. A $\theta_{\tilde{b}}$ independent limit cannot be set, but if $\theta_{\tilde{b}} = 0°$ then $M_{\tilde{b}} < 73\,\mathrm{GeV}/c^2$ providing $\Delta M_{\tilde{b}\chi} > 10\,\mathrm{GeV}/c^2$.

5.5 Search for Supersymmetry in Events with Photons and Missing Energy

It has recently been suggested that an unusual event observed at CDF[20] with two high energy electrons, two high energy photons and large amounts of missing energy might be due to the production of a pair of selectrons and their subsequent decay according to $\tilde{e}\tilde{e} \to ee\chi\chi \to ee\tilde{G}\tilde{G}\gamma\gamma$. This implies that the gravitino $\tilde{G}$ is the LSP, as predicted by the LNZ "no-scale supergravity" model[21] and gauge-mediated SUSY-breaking theories[22]. At LEP, we should therefore expect processes such as $e^+e^- \to \chi\chi \to \tilde{G}\tilde{G}\gamma\gamma$, leading to two acoplanar photons and missing transverse energy, and $e^+e^- \to \chi\tilde{G} \to \tilde{G}\tilde{G}\gamma$.

Searches are therefore performed for one or more energetic photons and missing energy[23]. Backgrounds arise from standard model production of $\nu\nu\gamma(\gamma)$ and $\gamma\gamma\gamma$ as well as cosmic rays etc. In the one-photon channel, 77 events are seen with an expected background of 82, leading to an upper limit on the cross-section which falls from 0.75 pb for a neutralino mass of $50\,\mathrm{GeV}/c^2$ to 0.4 pb at $160\,\mathrm{GeV}/c^2$. In the 2-photon channel, no candidates are detected, for an expected background of 0.9 and a selection efficiency of 69%. As shown in figure 14, this leads to a lower limit on the neutralino mass of $71\,\mathrm{GeV}/c^2$ for both the SUSY models considered.

5.6 R-parity Violating Supersymmetry

The discussion of supersymmetric models in this paper has so far assumed that R-parity is conserved. However, an R-parity-violating coupling may be added to the model, causing the LSP to be short-lived. The possible couplings are restricted by the need to avoid rapid proton decay. ALEPH has considered two cases, a lepton–lepton–slepton coupling (denoted LLE), and a lepton–quark–d-type-squark coupling (denoted LQD). In this scenario, the LSP will decay into standard model particles, while other SUSY particles may decay to S.M. particles either directly or through the LSP in a cascade. A number of topologies have been studied, involving many leptons, missing energy and multijets[24]. Results for an LLE coupling are translated into lower limits on the masses of charginos, neutralinos, sleptons, sneutrinos and squarks. For example charginos with masses less than $73\,\mathrm{GeV}/c^2$ and neutralinos less than $23\,\mathrm{GeV}/c^2$ are excluded for any generation structure of coupling, and for χ, $\tilde{l}$ or $\tilde{\nu}$ as the LSP.

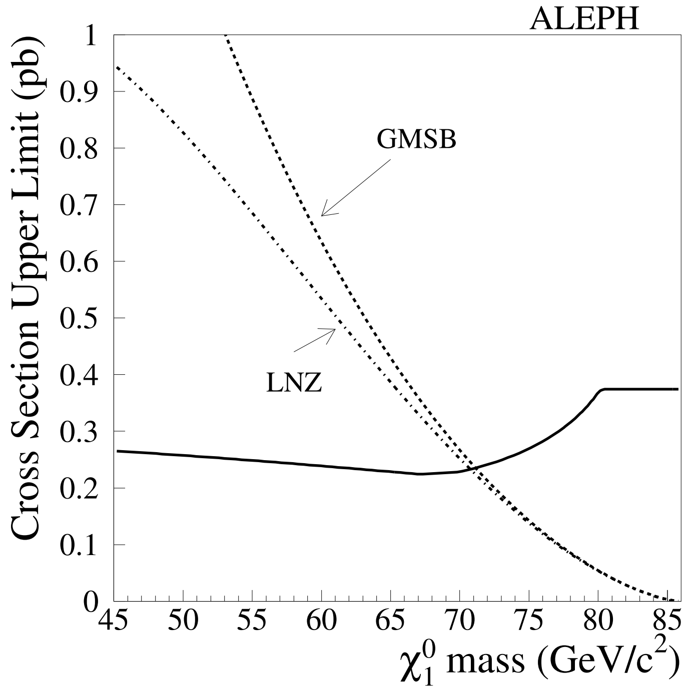

Figure 14: The 95% C.L. exclusion limit for χ compared with two $\tilde{\mathrm{G}}$ LSP theories.

6 Summary

ALEPH has obtained improved results in a number of areas by using the data collected at LEP 2. The mass of the W has been determined as $80.80 \pm 0.32 \pm 0.10\,\mathrm{GeV}/c^2$ by direct reconstruction, and $80.20 \pm 0.33 \pm 0.09\,\mathrm{GeV}/c^2$ from cross-section measurements at 161 and 172 GeV. The combined result is $M_{\mathrm{W}} = 80.51 \pm 0.24\,\mathrm{GeV}/c^2$, to be compared with the accepted value prior to LEP 2 of $80.33 \pm 0.15\,\mathrm{GeV}/c^2$[7]. Clearly, LEP results are now becoming competitive with those obtained at hadron colliders, and we look forward to improved values as the integrated luminosity increases. Studies of W decays have determined the CKM matrix element $|\mathrm{V_{cs}}| = 0.98 \pm 0.14 \pm 0.03$, and values of the triple gauge couplings have been seen to be consistent with the standard model.

Searches for Higgs particles have found no signal, and allowed limits to be placed of $M_{\mathrm{H}^0} > 74\,\mathrm{GeV}/c^2$, $M_{\mathrm{H}^\pm} > 52\,\mathrm{GeV}/c^2$, and $M_{\mathrm{h}} > 62.5\,\mathrm{GeV}/c^2$, all at the 95% confidence level. Supersymmetry searches have also found no evidence for physics outside the standard model, and have allowed limits to be placed for a large numer of SUSY particles. These include $M_\chi > 14\,\mathrm{GeV}/c^2$ ($M_\chi > 25\,\mathrm{GeV}/c^2$ for $\tan\beta > 1$, $M_{\tilde{\nu}} > 200\,\mathrm{GeV}/c^2$), $M_{\tilde{\mu}_{\mathrm{R}}} > 59\,\mathrm{GeV}/c^2$ providing $M_{\tilde{\mu}_{\mathrm{R}}} - M_\chi > 10\,\mathrm{GeV}/c^2$, and $M_{\tilde{\mathrm{t}}} > 67\,\mathrm{GeV}/c^2$ providing $\Delta M_{\tilde{\mathrm{t}}\chi}$ and $\Delta M_{\tilde{\mathrm{t}}\tilde{\nu}}$ are both over $10\,\mathrm{GeV}/c^2$. Supergravity models have also been tested, yielding a limit of $M_\chi > 71\,\mathrm{GeV}/c^2$ if $\chi \to \tilde{\mathrm{G}}\gamma$. Limits in the case of R-parity violating SUSY have also been obtained.

References

[1] ALEPH Collaboration, Nucl. Inst. and Meth. A294 (1990) 121.
[2] ALEPH Collaboration, Nucl. Inst. and Meth. A360 (1995) 481.
[3] ALEPH Collaboration, *W mass measurement through direct reconstruction in ALEPH*, presented at the International Europhysics Conference on High Energy Physics, 1997, Jerusalem.
[4] ALEPH Collaboration, Phys. Lett. B401 (1997) 347.
[5] D. Bardin, A. Leike, T. Riemann, Phys. Lett. B344 (1995) 383.

[6] ALEPH Collaboration, *Measurement of the W-pair cross-section in* e^+e^- *collisions at 172 GeV*, submitted to Phys. Lett. B.

[7] R.M. Barnett et al., Phys. Rev. D54 (1996) 1.

[8] ALEPH Collaboration, *Study of charm production in W decays*, presented at the International Europhysics Conference on High Energy Physics, 1997, Jerusalem.

[9] ALEPH Collaboration, *Measurement of the triple gauge-boson couplings at 172 GeV*, presented at the International Europhysics Conference on High Energy Physics, 1997, Jerusalem.

[10] ALEPH Collaboration, *Search for the standard model Higgs boson in* e^+e^- *collisions at 161, 170 and 172 GeV*, submitted to Phys. Lett. B.

[11] Y.L. Dokshitzer, J. Phys. G17 (1991) 1441.

[12] ALEPH Collaboration, Phys. Lett B384 (1996) 427.

[13] ALEPH Collaboration, *Search for charged Higgs bosons in* e^+e^- *collisions at centre-of-mass energies from 130 to 172 GeV*, submitted to Phys. Lett. B.

[14] ALEPH Collaboration, *Search for the neutral Higgs boson of the MSSM in* e^+e^- *collisions at* $\sqrt{s}$ *from 130 to 172 GeV*, submitted to Phys. Lett. B.

[15] ALEPH Collaboration, *Searches for charginos and neutralinos in* e^+e^- *collisions at* $\sqrt{s} = 161$ *and 172 GeV*, submitted to Z. Phys. C.

[16] ALEPH Collaboration, Phys. Lett. B407 (1997) 377.

[17] K. Inoue et al, Prog. Theor. Phys. 68 (1982) 927; 71 (1984) 43;
H.P. Nilles, Phys. Rep. 110 (1984) 1;
H.E. Haber and G.L. Kane, Phys. Rep. 117 (1985) 75.

[18] ALEPH Collaboration, *Implications of ALEPH SUSY searches for the MSSM*, presented at the International Europhysics Conference on High Energy Physics, 1997, Jerusalem.

[19] ALEPH Collaboration, *Searches for scalar top and scalar bottom quarks at LEP 2*, submitted to Phys. Lett. B.

[20] S. Park, *Proceedings of the 10th Topical Workshop on Proton-Antiproton Physics,* page 62, AIP, New York, 1995.

[21] J. Lopez and D. Nanopoulos, Phys. Rev. D55 (1997) 4450.

[22] S. Dimopoulos et al., Phys. Rev. Lett. 76 (1996) 3498.

[23] ALEPH Collaboration, *Search for supersymmetry in the photon(s) plus missing energy channels at* $\sqrt{s} = 161$ *GeV and 172 GeV*, submitted to Phys. Lett. B.

[24] ALEPH Collaboration, *Searches for R-parity violating supersymmetry at LEP II*, presented at the International Europhysics Conference on High Energy Physics, 1997, Jerusalem.